Malaysian Journal of Chemistry, 2026, Vol. 28(4), 75-88

Bio-Based Eugenol-Benzoxazine/Polyurethane Copolymers as High-Performance Corrosion Inhibitor Coatings for Mild Steel: Synthesis, Characterization, and Electrochemical Evaluation

Elavarasan, S.[1]*, Vijayakumari, N.[2] and Anbuselvi, D.[3]
[1]Department of Chemistry, Muthayammal Engineering College (Autonomous), Namakkal, India
[2]Department of Chemistry, Government Arts College for Women, Salem, India
[3]Department of Physics, T. John Institute of Technology, Bangalore, India
*Corresponding author (e-mail: prince2chem@gmail.com)

A novel eugenol-based benzoxazine monomer (EuBz-ada) was synthesized via the reaction of paraformaldehyde, 3-amino-5-methylisoxazole, and eugenol, and its structure was confirmed by proton NMR, FT-IR, and UV-visible spectroscopy. The resulting monomer and its polyurethane-based copolymers were tested as corrosion inhibitors for mild steel; electrochemical polarization and electrochemical impedance spectroscopy (EIS) studies showed that the coatings containing EuBz-ada and different concentrations of polyurethane (PU) significantly increased corrosion resistance. Inhibition efficiency increased with PU content, confirmed by computational investigations using density functional theory (DFT), which suggested strong adsorption and favourable electronic properties. Further investigations showed a decrease in water absorption and an increase in gel content for the copolymeric coatings, which was in line with superior barrier properties. These results indicate the potential of bio-based EuBz-ada/polyurethane systems as effective and environmentally friendly corrosion inhibitors for mild steel protection.

Keywords: Eugenol-benzoxazine, polyurethane copolymer, corrosion inhibitor, mild steel, bio-based coating

Received: January 2026; Accepted: April 2026

Steel's vulnerability to corrosive media has resulted in significant financial losses and possible risks [1]. Currently, one of most successful techniques for the prevention of corrosion is the application of organic resin coatings on metal surfaces. As previously stated [2-6], polybenzoxazines, an original type of phenolic resin, maintain exceptional mechanical qualities, including strong dielectric properties, high char yield, minimal water absorption, as well as nearly zero shrinkage upon curing. They can be used to manufacture corrosion-resistant materials because of these appealing qualities. Materials, particularly metals, could be destroyed by chemical as well as electrochemical reactions with their environment during the natural process of corrosion. Corrosion is estimated to cost the global economy more than $2.5 trillion annually [1]. Because of their superior mechanical properties, affordability, and accessibility, metals such as carbon steel are employed extensively in the industrial sector [5]. However, conducting polymers have drawn increasing attention as protective coatings and film-forming corrosion inhibitors because of their notable anti-corrosion qualities and environmental friendliness [6]. By creating a barrier layer, organic coatings commonly stop corrosion on metal surfaces. Their high electron density from heteroatoms such as nitrogen, oxygen, sulfur, and aromatic rings makes them effective anti-corrosion inhibitors for mild steel (MS) under various corrosive conditions [7-14]. Because of its low dielectric constant, minimal water absorption, as well as its strong resistance to heat and chemicals, polybenzoxazine (PBZ) is a potential corrosion prevention material [15, 16].

Compared to similar amines and aldehydes, Schiff bases with aromatic rings as well as –C=N- groups in their molecular structure have been shown to be superior corrosion inhibitors [17]. By adhering to the surface of Q235 steel, a chitosan salicylaldehyde Schiff base was demonstrated to prevent corrosion [18]. Another study discovered that chitosan vanillin material prevented MS from corroding by the formation of a protective layer on its surface, utilising AFM as well as WCA analysis [19]. Furthermore, polybenzoxazine was utilized in a number of applications, such as antifouling and anticorrosion coatings [8, 20], high flame retardancy polymers [21], as well as high voltage insulation materials [22]. It is an ideal option for creating carbon structures with catalysis applications that go beyond energy as well as the environment. Because of its high char production after carbonization, it is used in carbon compounds [23]. Although polybenzoxazine coatings have shown promising properties, most studies focus on petrochemical-based benzoxazines or do not systematically address environmental concerns. Furthermore, many of the reported benzoxazine-based inhibitors achieve significant corrosion protection only at relatively high loading levels, thus limiting their practical application. Therefore, new bio-based benzoxazine systems that exhibit high inhibition efficiency at low concentrations and eco-friendliness are highly desirable.

Currently, two methods have been proposed to soften polybenzoxazine coatings: adding plastic polymers or nanofiller (such as carbon nanotube) to polybenzoxazine [24], adding flexible silane or alkyl long-chain segments to the backbones or branched chains of benzoxazine monomers [25, 26]. The goal of such work is to use molecular design to include an efficient Schiff base moiety in a benzoxazine precursor. Polybenzoxazine coatings, such as poly (SF-Tol-BZ) coatings, are being developed to reduce corrosion in MS. Open circuit potential (OCP), electrochemical impedance spectroscopy (Nyquist and Bode plots) and potentiodynamic polarization (Tafel curves) are among methods used to evaluate the efficacy of these coatings in the maritime environment. Over the past few years, bio-based polybenzoxazine has garnered significant attention in academia due to the mounting pressure of environmental contamination [27, 28]. Eugenol [8, 15], pyrogallol, cardanol, urushiol [13], stearylamine [14], furfurylamine [12, 16] and other renewable raw materials were used to create bio-based polybenzoxazines. Among other bio-based polymers, polyurethane (PU) was chosen as the copolymer matrix, because of its flexibility, high mechanical strength, strong adhesion to metal substrates, and good barrier properties against water and corrosive agents. Although other bio-based polymers such as polylactic acid, chitosan, and cellulose derivatives have been studied for anticorrosion applications, they are typically brittle, have poor film-forming ability, and lack chemical resistance, which can limit their long-term protection [8, 12, 13, 15]. In the present study, we have synthesised bio-based EuBz-ada/polyurethane anticorrosion inhibitors and analysed their inhibition properties on mild steel using experimental and DFT methods.

EXPERIMENTAL

Chemicals and Materials

Infrared spectra were recorded with a Thermo Logical Nicolet iS50 FT-IR spectrometer, and UV spectra with a Labman LMSP UV-1200 UV-Vis spectrometer. ^{1}H NMR was performed using a Bruker 500 MHz instrument with DMSO-D_6 as the solvent. The polarization measurements were performed using a typical three-electrode cell. Ag/AgCl served as a reference electrode, while platinum served as the counter electrode. A Biologic SP 300 type electrochemical workstation was used to detect potentiostatic polarization. Water absorption tests were performed as per ASTM D570, by immersing coated mild steel samples in distilled water at 25 °C for 24 hours, removing the specimens, wiping them with a cloth to remove surface water, and weighing them again to determine water uptake as a percentage of the initial weight.

Computational Details

Calculations of DFT with a hybrid functional B3LYP (Becke's three-parameter hybrid functional using the BLYP correlation functional) and the 6-311G(d) basis set basis set using the Berny method were performed with the Gaussian 09W program [29]. No symmetry constraints were applied during geometry optimization. The physical characteristics used in the optimization of the molecular structures of the proposed structure were (σ) absolute softness (χ) electronegativities, electronic charge, (η) absolute hardness, (ω) global electrophilicity, (S) global softness, and (Pi) chemical potential. These were calculated using the following equations [30-34]:

$$IE = -EHOMO \quad (1)$$

$$EA = -ELUMO \quad (2)$$

$$\chi = -\frac{IE+EA}{2} \quad (3)$$

$$\eta = \frac{IEE-A}{2} \quad (4)$$

$$\omega = \frac{\mu^2}{2\eta} \quad (5)$$

$$\Delta N_{max} = \frac{IE+EA}{2(I-A)} \quad (6)$$

$$\omega^+ \approx (IE+3EA)^2/(16(IE-EA)) \quad (7)$$

$$\omega^- \approx (3IE+EA)^2/(16(IE-EA)) \quad (8)$$

$$\Delta\varepsilon_{back-donation} = -\frac{\eta}{4} \quad (9)$$

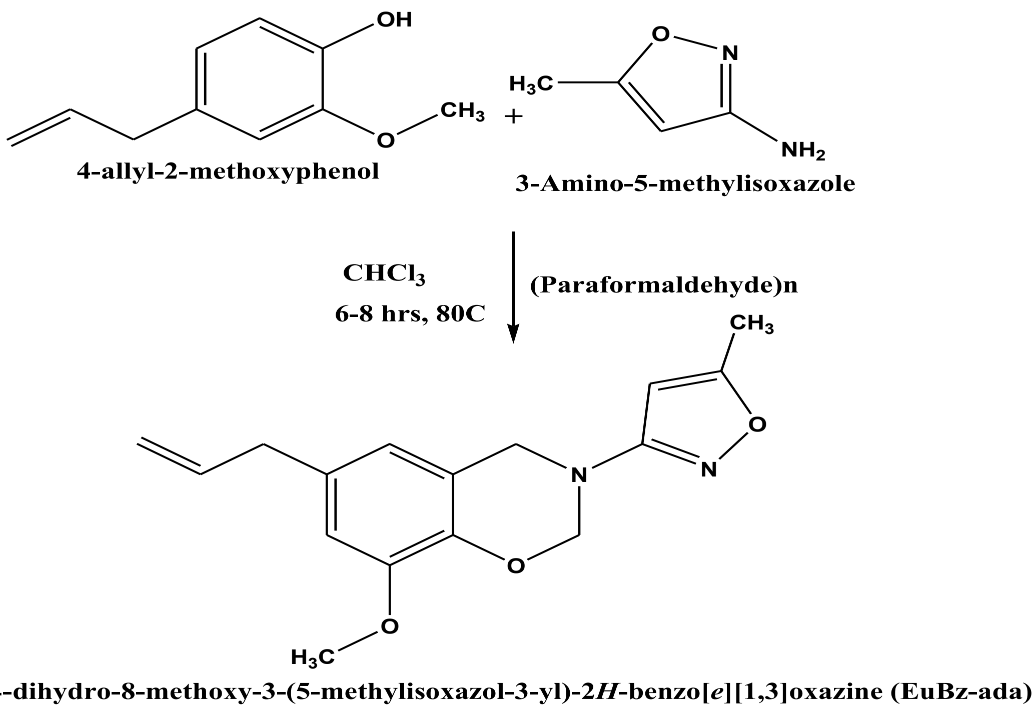

Scheme 1. Synthesis of the EuBz-ada monomer.

Synthesis of EuBz-ada Monomer 6-allyl-3,4-dihydro-8-methoxy-3-(5-methylisoxazol-3-yl)-2H-benzo[e][1,3]oxazine

All chemicals were purchased from Sigma-Aldrich and were used as received, without any additional purification. After dissolving paraformaldehyde (0.365 g, 12 mmol) and 3-amino-5-methylisoxazole (0.926 mL, 9.5 mmol) in 20 mL of chloroform, the mixture was shaken for 30 minutes at 50 °C. Eugenol (1 g, 6.09 mmol) and more chloroform (80 mL) were added, and the mixture was refluxed for 24 hours at 80 °C [35]. TLC was utilised to track the reaction progress. After the reaction was complete, chloroform (100 mL), 1 N sodium hydroxide (200 mL), double distilled water (100 mL), and sodium chloride (100 mL) solution were added to the original mixture. The organic layer was separated and dried over anhydrous sodium sulfate. Finally, the EuBz-ada monomer was extracted from the dried organic layer. The following crude monomer was utilized to further synthesise polymeric polymers with isocyanate. A solution containing a certain ratio of isocyanate hardener in toluene was used to re-dissolve this synthetic monomer in 1,4-dioxane. Three different EuBz-ada monomers as well as isocyanate composites, EuBz-ada-PU100:60, EuBz-ada-PU100:80, and EuBz-ada-PU100:100, were prepared by varying the isocyanate content by 60, 80, and 100 in relation to the monomer quantity.

Coating and Curing

The MS plate was sequentially cleaned with acetone, hexane, and water to remove impurities prior to coating, and was further enhanced with surface roughening using Emery paper. The polymer coating was then applied to the MS plate using a dip-coating method followed by thermal curing. Three formulations of the coating liquid were prepared by mixing the monomer with different amounts of isocyanate hardener in a 7:3 mixture of 1,4-dioxime and toluene. The MS plate was immersed in the polymer solution for 1 min and then withdrawn at a speed of 100 mm/min. The coated samples were thermally cured in a furnace at 200 °C for 3 hours. The viscosity of the polymer solution was characterized before coating and controlled at 50 cP using a Brookfield viscometer. The withdrawal speed of 100 mm/min was chosen based on preliminary trials which showed that this speed resulted in coatings that were uniform and free from sagging or streaking. Coating uniformity was verified by measuring the film thickness at five locations on each substrate, as well as by optical microscopy. The curing conditions (200 °C for 3 hours) were selected from literature reports [35, 36] and further validated by preliminary experiments in this study, which showed that this protocol yielded coatings with adequate adhesion and mechanical strength without thermal degradation. The corrosion resistance of the coated samples was evaluated by electrochemical analysis.

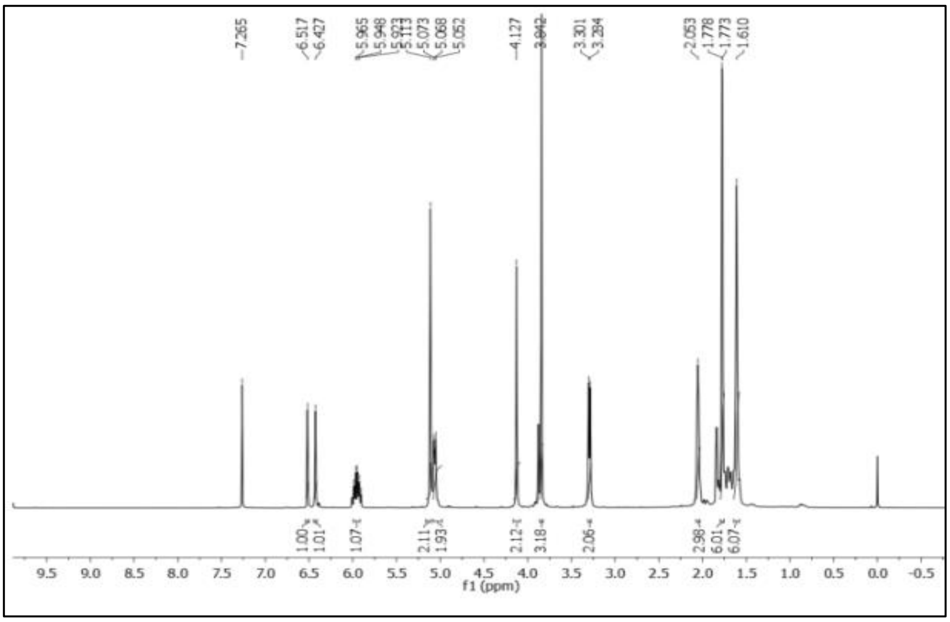

Figure 1. ^{1}H NMR spectrum of EuBz-ada monomer.

RESULTS AND DISCUSSION

NMR Analysis of EuBz-ada Monomer

The monomer structure was confirmed by ^{1}H NMR spectrometry. EuBz-ada, ^{1}H NMR (500 MHz, DMSO-D_6, ppm): 7.26 (2H, d, Ar-H), 6.51 (1H, s), 4.12 (2H, s, HC=CH), 3.30-3.28 (4H, d, NCH_2), 2.05 (2H, s, CH_2), 3.94 (3H, s, OCH_3), 1.77-1.61 (3H, t, CH_3). The ^{1}H NMR spectrum exhibited aromatic proton bands at 7.26 ppm (2H), consistent with the proposed structure. These results clearly indicate that the synthesized monomer possessed the expected structure, as depicted in Figure 1 [35].

FT-IR Analysis of Pure EuBz-ada and EuBz-ada Blends with PU

The FT-IR spectra obtained are displayed in Figure 2. FT-IR analysis was utilised to identify functional groups present in the samples. The spectrum of the monomer exhibited characteristic absorption bands at 2988 and 2976 cm^{-1} (υsymCH_3), 2875 and 2864 cm^{-1} (υsymCH_3), and 1714 cm^{-1} (υC=O stretching). Bands were observed at 1544, 1512, 1488, and 1486 cm^{-1} (υC=C); 1244 cm^{-1} (υC=N); 1202 and 831 cm^{-1} (C–O stretching); and 1312, 1254, 1226, and 1018 cm^{-1} (γCH bending). Out-of-plane CH bending vibrations were present at 918, 815, and 741 cm^{-1}.

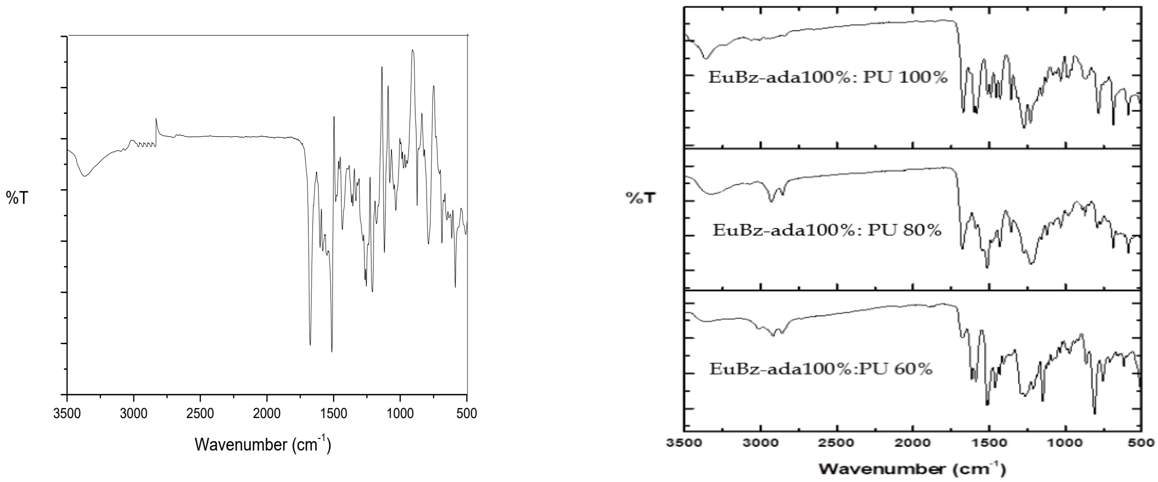

Figure 2. FT-IR spectra of (a) EuBz-ada and (b) EuBz-ada blends with PU.

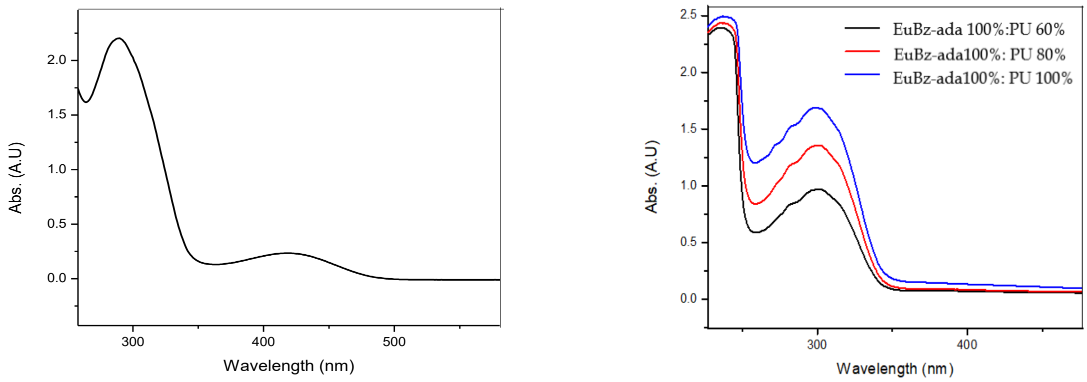

Figure 3. UV-Visible spectra of (a) EuBz-ada and (b) EuBz-ada blends with PU.

UV Analysis of Pure EuBz-ada and EuBz-ada Blends with PU

Electronic spectroscopy, sometimes called UV-visible spectroscopy, analyses the electronic transition of organic compounds. The UV-visible spectra of the monomer and polymer composites obtained in room temperature water are displayed in Figure 3.

The UV-visible spectrum of EuBz-ada had two absorption bands at 292 and 315 nm. π-π* as well as n-π* transitions of EuBz-ada were responsible for these absorbance bands. The bands moved to the redshift region when polyurethane was added to EuBz-ada. The absorbances of EuBz-ada:PUs were detected at 302 nm and 328 nm. A low energy Intramolecular Charge Transfer (ICT) π-π* transition is indicated by the absorbance at 328 nm, which is consistent with earlier observations of benzoxazine. Additionally, the band corresponding to an n-π* transition increased in absorbance, indicating that polyurethane significantly triggered the monomer's electronic transition. This suggests that the produced copolymers may exhibit greater corrosion resistance.

Potentiodynamic Polarization

The synthesized 6-allyl-3,4-dihydro-8-methoxy-3-(5-methylisoxazol-3-yl)-2H-benzo[e][1,3]oxazine (EuBz-ada) was evaluated for its corrosion inhibition performance using potentiodynamic polarization measurements (Fig. 4 and Table 1). The polarization curves of the blank and EuBz-ada with different concentrations (60 %, 80 %, and 100 %) showed clear shifts in both anodic and cathodic branches compared to the blank, which is indicative of mixed-type inhibition with predominantly cathodic control. The E_{corr} values shifted toward a more negative value due to the addition of EuBz-ada and its blends, and the mixed-type inhibition mechanism was confirmed by the variations in the anodic and cathodic branches, and by the more pronounced suppression of the cathodic current density. This suggests that the inhibitor had a stronger effect on a cathodic reaction such as the hydrogen evolution reaction, while still hindering the anodic dissolution of iron. The IE % calculated from the polarization curves increased with inhibitor concentration, suggesting that a physical barrier was formed, reducing the active surface area for electrochemical reactions. The Tafel slopes (βa and βc) showed slight deviations, suggesting that the inhibition mechanism did not change the nature of the corrosion process, but rather hindered the kinetics of electron transfer at the anodic and cathodic sites.

Here, $I_{corr}(b)$ represents the corrosion current for an uncoated MS plate, $I_{corr}(c)$ represents the corrosion current for the EuBz-ada: PU coated MS plates.

$$\text{Corrosion rate} = (I_{corr} \times K \times EW)/\rho Ammpy\ 1 \qquad (1)$$

Here, K=3272 mm year^{-1} (rate constant), equivalent weight of mild steel = 27.9 g

Mild steel density = 7.85 g cm^{-3}, A (area of sample) = 1 cm^{2}

$$\text{Corrosion efficiency (\%)} = [(I_{corr}(b) - I_{corr}(c))/(I_{corr}(b))] \times 100 \qquad (2)$$

Table 1. Potentiodynamic polarization parameters for mild steel in NaCl, in the absence and presence of different concentrations of inhibitors (Bz-ada:PU), at room temperature.

Concentration of Sample (EuBz-ada:PU)	Tafel studies						
	Icorr (mA)	Ecorr (mV)	Tafel constant mv/decade		Corrosion Efficiency (%)	Surface Coverage (θ)	Corrosion Rate (mmpy)
			b_a	b_c			
Blank	4.87	-514.18	119.20	435.80	-	-	56285.06
100:60	1.663	-498.26	177.19	106.78	65.85	0.6585	19339.27
100:80	1.167	-482.03	84.75	211.50	76.03	0.7603	18722.92
100:100	0.122	-560.98	42.50	83.92	97.48	0.9748	1418.75

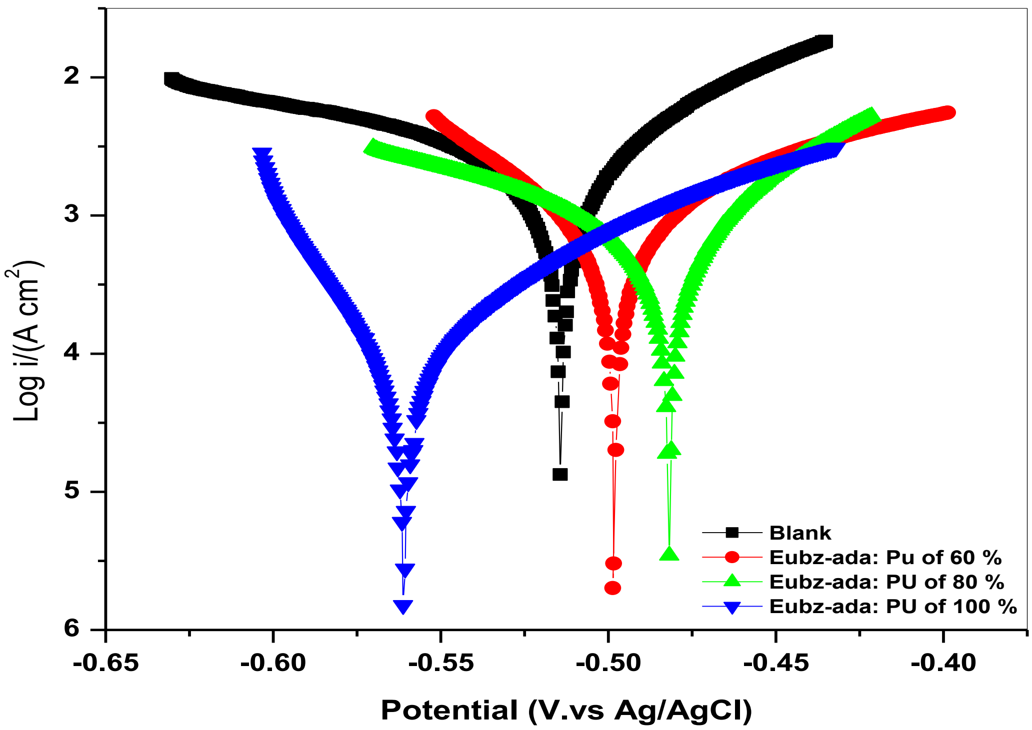

Figure 4. Tafel curves for mild steel with variable concentrations of EuBz-ada.

Electrochemical Impedance Spectroscopy (EIS)

These findings are consistent with the polarization studies (Figure 5), where the EIS measurements showed depressed semicircles for all samples, typical of corrosion processes controlled by charge transfer. The diameter of the semicircle [37-39], which represents the charge transfer resistance (Rct), became larger with increasing EuBz-ada concentration. The 100% EuBz-ada sample showing the largest semicircle, the highest Rct and hence best inhibition performance. This was also confirmed by the increase of Rct with inhibitor concentration and the decrease of the double-layer capacitance (Cdl) with increasing inhibitor concentration. This suggests that the EuBz-ada effectively suppressed the electrochemical reactions at the metal/solution interface by forming a protective layer that displaced water molecules and decreased the local dielectric constant. This was facilitated by the adsorption of EuBz-ada molecules onto the surface, as indicated by the presence of heteroatoms (N, O) and aromatic rings in the EuBz-ada molecule, which can interact with the metal through π-electron donation and lone pair electrons.

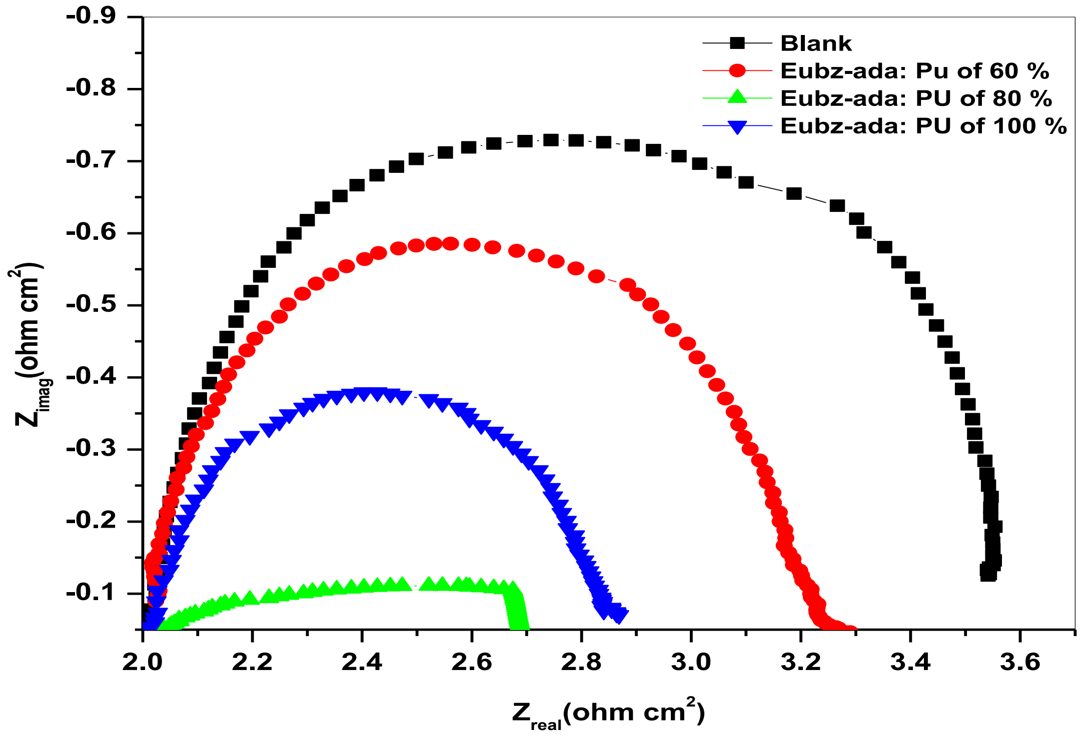

Figure 5. EIS for blank and various amounts of EuBz-ada on mild steel.

Adsorption and Surface Protection Mechanisms

The highly efficient inhibition performance of EuBz-ada can be attributed to its chemical structure, which contains multiple adsorption centres, including nitrogen, oxygen, and the aromatic rings. These functionalities facilitate strong adsorption onto the metal surface via coordinate bonds and π-electron interactions, displacing water molecules and forming a compact, adherent protective film. The efficiency data suggest that the adsorption of EuBz-ada follows Langmuir adsorption behaviour, which was confirmed by the linear plot of C/θ versus C (where θ is the surface coverage). The calculated adsorption equilibrium constant (K_{ads}) and standard free energy of adsorption (ΔG°_{ads}) values indicate spontaneous and strong adsorption, consistent with chemisorption.

The superior inhibition efficiency of the EuBz-ada/polyurethane system can be attributed to the presence of heteroatoms such as nitrogen and oxygen in the molecular structure. These atoms possess lone pairs of electrons that can coordinate with vacant d-orbitals on the Fe surface, resulting in strong chemisorption and the formation of a protective inhibitor layer. Such coordination is well-supported in the literature [8, 9, 12, 35], and plays a crucial role in enhancing both the adsorption strength and inhibition efficiency of organic inhibitors containing N, O, and aromatic moieties.

Structure–Activity Relationship

The higher level of inhibition by EuBz-ada at 100% compared to EuBz is due to the electron-donating isoxazole and benzo[e][1,3] oxazine rings and the methoxy and allyl substituents, which interact with vacant d-orbitals on the metal surface and create a thicker, more protective, and more electron-donating inhibitor film, maximizing surface coverage and film stability.

Practical Implications and Comparative Performance

The combined potentiodynamic and EIS results revealed that EuBz-ada was an effective corrosion inhibitor for the studied system, with inhibition efficiencies much higher than those of conventional inhibitors at relatively low concentrations. This indicates its potential for practical application in industrial corrosion protection. In addition, the precursor molecules for EuBz-ada preparation are environmentally friendly, and the synthesis conditions are mild (Scheme 1), thus making EuBz-ada an eco-friendly corrosion inhibitor. The inhibition mechanism of EuBz-ada includes mixed-type behaviour, strong adsorption, and effective inhibition of both anodic and cathodic reactions, which will guide the design of new, high-performance, and green corrosion inhibitors.

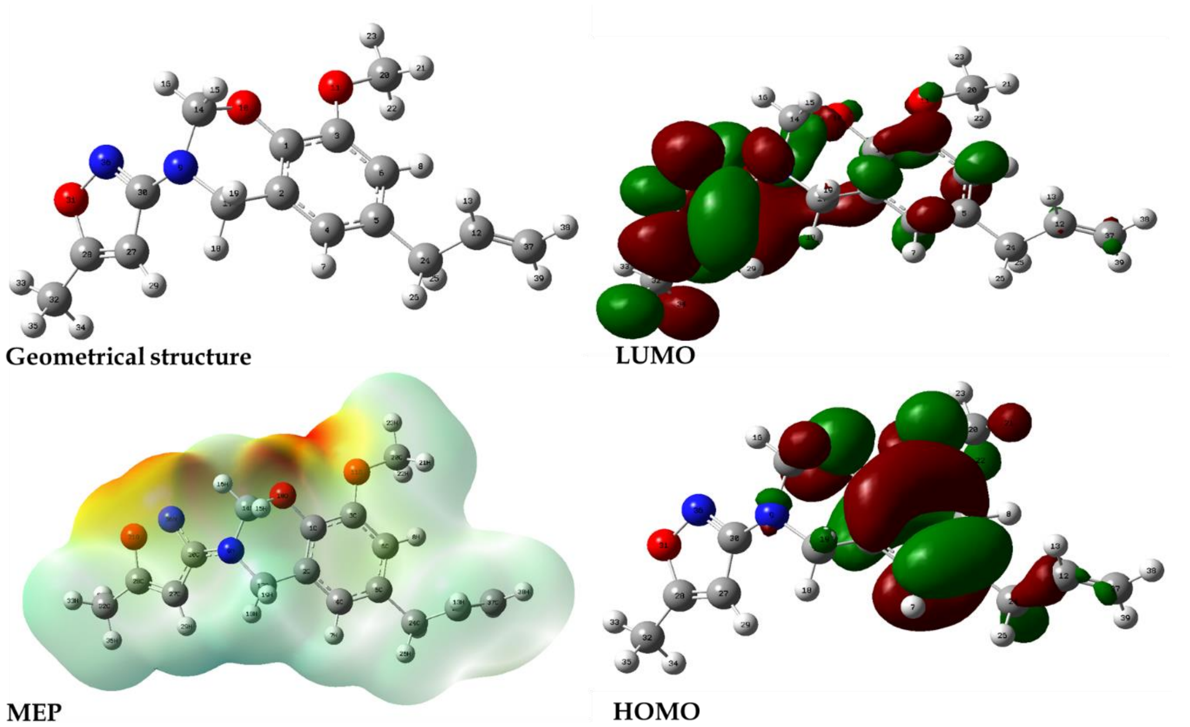

Figure 6. The frontier molecular orbitals (EHOMO, ELUMO), geometric structure and MEP images of EuBz-ada.

The environmentally friendly claim of the developed coating is attributed to the use of eugenol, a naturally occurring phenolic compound extracted from clove oil, as the renewable raw material for benzoxazine synthesis, which reduces dependency on petroleum-based feedstocks and minimizes the environmental footprint. The synthesis route does not require hazardous reagents and proceeds under relatively mild conditions. While these are not specifically addressed in this performance study, they represent important benefits over traditional benzoxazine systems, which are typically derived from petrochemical sources and often employ more toxic chemicals.

Theoretical Calculations

The density functional theory (DFT) is the most popular quantum chemical analysis [40-43] that has been used to study the interactions between metal surfaces and corrosion inhibitors. Because of time, cost, and ecological implications, as well as the inadequacy of conventional methods, the application of computational studies to investigate metal corrosion inhibition has skyrocketed. With this technique, the degree of corrosion inhibition of a polymeric compound can be obtained by determining its chemical reactivity. Computations of molecular and electronic properties were performed to fully understand the corrosion protection system provided by specific molecules; these results are presented in Table 2 and provide evidence that these inhibitors adsorb favourably and provide corrosion protection. Fig. 6 shows the optimized geometries and HOMO-LUMO plots of the newly synthesized EuBz-ada ionic liquids. The physicochemical parameters were calculated in the gaseous phase and aqueous (water) phase. The lowest HOMO-LUMO gap was observed for EuBz-ada (5.31 eV in the aqueous phase and 5.33 eV in the gaseous phase), which indicates its higher reactivity potential and efficacy as an electron or charge donor and acceptor. The dipole moment (μ) values (which are compared in D) also support these distinctions. Electronegativity (χ) results demonstrated that EuBz-ada was the most electron-attractive. Global hardness (η) results also indicated that EuBz-ada was the hardest (2.654 eV), and therefore the most reactive, which is consistent with the interpretation of band gap. The electrophilicity index (ω) demonstrated a meaningful capability to receive electrons and participate with electrophiles. These descriptors suggest that EuBz-ada may be a very chemically active and polarizable system, with interactions with electron rich. The detailed insights into E_{HOMO}, E_{LUMO}, ΔE, IP, EA, dipole moment, electronegativity, hardness, softness, and ΔN collectively contribute to unravelling the molecular mechanisms governing the inhibitory action of EuBz-ada, paving the way for their application in real-world scenarios related to corrosion protection and beyond. Finally, the quantum chemical parameters (HOMO-LUMO gap and electronegativity) calculated for EuBz-ada showed its high reactivity and strong adsorption potential on the steel surface, leading to efficient donor-acceptor interactions and strong surface adsorption, thus contributing to the high corrosion inhibition efficiency in electrochemical experiments (see Table 2).

Water Adsorption Studies

The development of anti-steel corrosion products is significantly influenced by the hydrophobic character of polymeric materials. The hydrophobic characteristics of polymeric materials may be influenced by their densities of branching and cross-linking. The coating's binder activity also has an impact on this property, resulting in the creation of materials with a larger cross-density polymer content and more potent hydrogen bonding ability. Therefore, the urethane content may improve the hydrophobic properties of the polymer, which could result in more urethane-containing polymers having lower water adsorption than their competitors. Figure 7. shows the water absorption of the monomer and polymeric complexes. The amount of water diffusion in the monomer alone (1.89 %) was less than previously reported. The novelty of the present work is the design of a eugenol-derived benzoxazine monomer functionalized with an adamantane group and copolymerized with polyurethane, which integrates the inherent hydrophobic and structural properties of adamantane with the flexibility and enhanced barrier properties of polyurethane. The EuBz-ada/polyurethane system exhibited improved water resistance, gel content, and corrosion inhibition efficiency at lower additive concentrations compared to previous bio-based benzoxazine coatings, and the use of renewable resources and the synergistic effect between EuBz-ada and polyurethane represents a significant improvement over prior work.

Table 2. Quantum parameters of EuBz-ada.

Solvent	HOMO	LUMO	IP	EA	ΔE	c	µ	h	σ	w	e	w+	Dipole Moment	Toal Energy
Gaseous Phase	-5.564	-0.234	5.564	0.234	5.329	-2.899	-2.899	2.665	0.375	1.577	0.634	0.034	5.12	-955.341
Aqueous Phase (Water)	-5.787	-0.478	5.787	0.478	5.308	-3.132	-3.132	2.654	0.377	1.848	0.541	0.070	7.38	-955.355

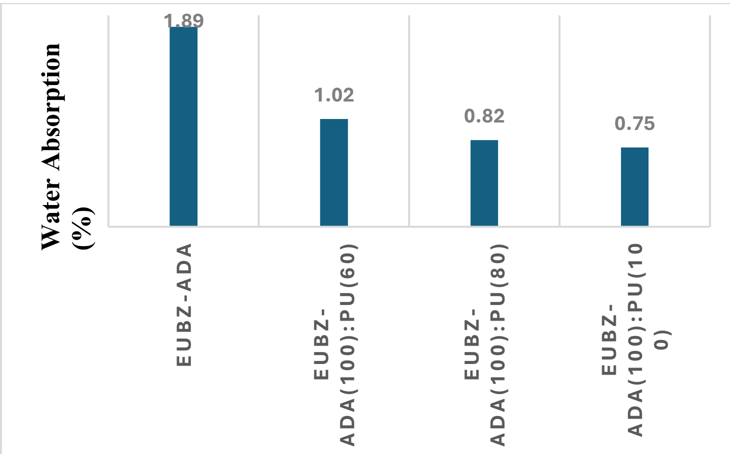

Figure 7. The water absorption % of the EuBz-ada monomer.

The adamantane ring, which makes the entire molecule more hydrophobic, may be the cause of this wonderful result. As more urethane was added to the polymeric material, the percentage of water diffusion fell; for EuBZ-ada:PU 100, this percentage extent a maximum of 0.75%. This study shows that the urethane and adamantane rings' physical characteristics greatly enhanced water diffusion. The following formula was utilised to calculate the water absorption percentage [35, 42]:

Percentage of water absorption = [(Wa-Wb)/Wb] x 100 `(1)

where,

Wa = Weight of coated mild steel after exposure to water absorption

Wb = Weight of coated mild steel before exposure to water absorption

Gel Content

Gel formation is an important factor that may have a correlation with water diffusion investigations. More gel formation and less water diffusion results from materials that can build stronger intra-linkages between themselves, which can also decrease the molecule's porosity. From this point on, every polymeric and monomeric substance was analyzed, and the outcomes are shown in Fig. 8. The amount of urethane significantly increased the gel-forming ability of the monomer EuBZ-ada, which was almost 83.62 %. There was 92.13 % gel formation in the 100 % urethane. All polymeric materials might potentially possess anti-corrosive properties, as proved by the superior gel creation of all compounds except the monomer. The subsequent formula was utilised to evaluate the coating's gel content [35, 42]:

Percentage of gel content = (Wa/Wb) x 100 (2)

where Wa and Wb are the weights of coated mild steel after and before extraction, respectively.

Microscopic Analysis

As with any corrosion investigation, the environment of focus must be carefully chosen. Maximizing thermal presentation and component lifespan (by limiting corrosion product release and environmental deterioration) is the aim of choosing the water chemistry for a nuclear reactor. Erosion affects not just the economy but also the environment, security, and well-being. Consumption affects all initiatives, including those involving assets, oil and gas, and most human activities. In this study, the 60, 80, and 100 PU in 3.5% NaCl-created polymeric materials showed significant erosion relief both before and after loading the monomer (Fig. 9). Notably, corrosion significantly decreased as a result of adding more polyurethane. Tests on EuBZ-ada:PU100-60, for example, showed an advanced surface after consumption related to the untreated sample, while tests on EuBZ-ada:PU100-80 showed further development in the example covered with 80% polyurethane. Furthermore, compared to its pre-consumption state, the specimen coated with 100% polyurethane exhibited nearly no roughness on the delicate steel surface.

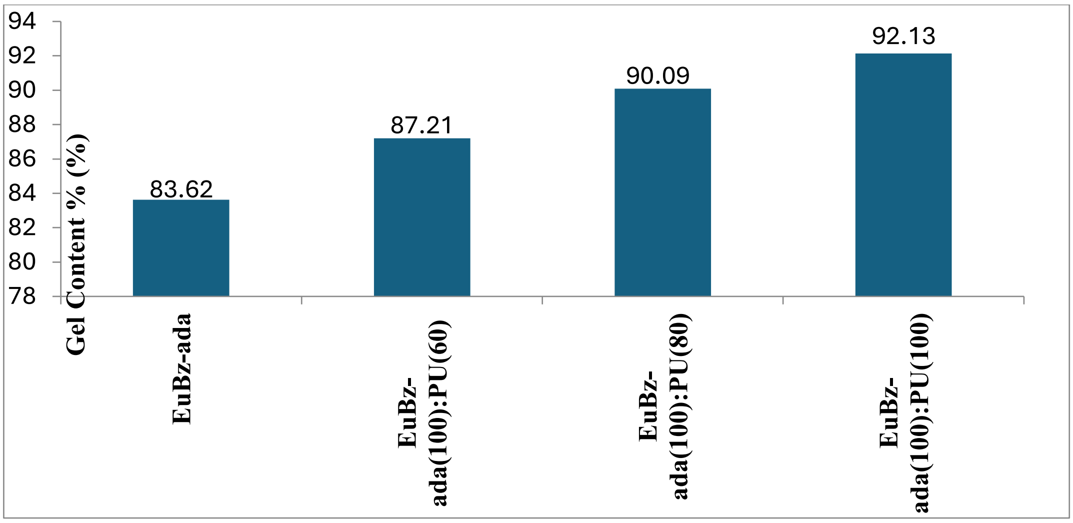

Figure 8. Gel absorption of EuBz-ada and EuBz-ada blends with PU.

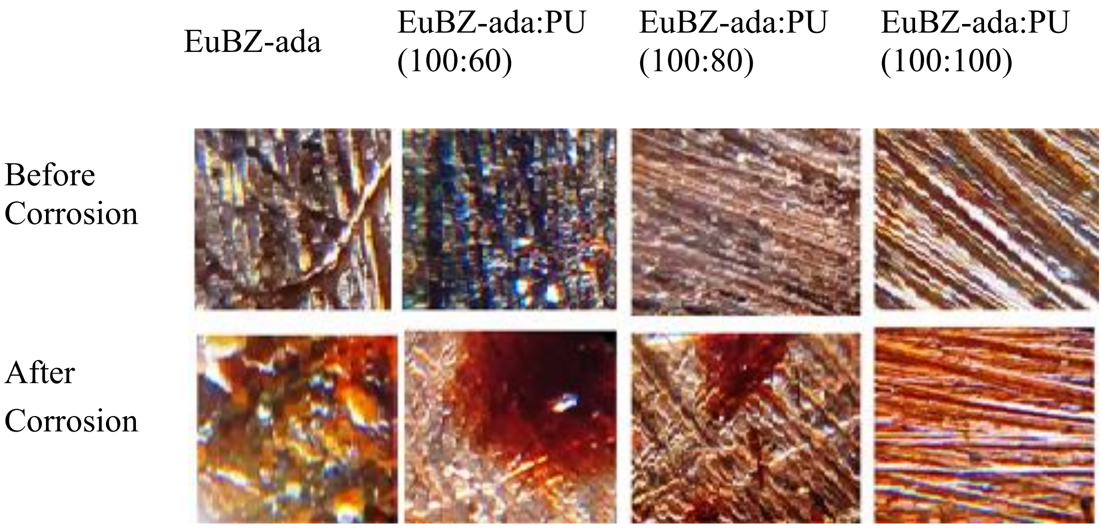

Figure 9. Microscopic images of EuBz-ada-PU copolymers before and after immersion in 3.5% NaCl.

CONCLUSION

In this study, we integrated a monomer concentrated on benzoxazine with a very hydrophobic adamantane platform. A new eugenol-derived benzoxazine (EuBz-ada) and its copolymers were reacted with polyurethane (PU) to obtain high-performance, bio-based anti-corrosion coatings for mild steel. These were comprehensively characterized, and the developed copolymers were tested electrochemically and showed significantly enhanced corrosion inhibition efficiency, water resistance, and gel content, compared to the monomer and to reported bio-based alternatives. This is attributed to the combined effects of the hydrophobic adamantane group and the barrier and flexible properties of PU, which led to robust, adherent, and durable coatings. The use of renewable eugenol and environmentally benign synthesis conditions further enhances the eco-friendly nature of the developed system. The EuBz-ada/PU coatings showed high inhibition efficiencies at relatively low additive concentrations and have good potential to serve as a sustainable alternative to petroleum-based inhibitors. Theoretical (DFT) studies confirmed the strong adsorption and high reactivity of the developed copolymers toward steel surfaces. Overall, the results indicate the practical potential of EuBz-ada/PU copolymers for industrial corrosion protection applications. Future work will be dedicated to the environmental assessment, long-term performance, and optimization of the formulation for increased substrate compatibility.

REFERENCES

1. Al-Amiery, A. A., Isahak, W. N. R. W. and Al-Azzawi, W. K. (2023) Corrosion inhibitors: natural and synthetic organic inhibitors. *Lubricants*, **11**, 174. https://doi.org/10.3390/lubricants11040174.

2. Caldona, E. B., Al-Christopher, C., Pajarito, B. B. and Advincula, R. C. (2017) Novel anti-corrosion coatings from rubber-modified polybenzoxazine-based polyaniline composites. *Applied Surface Science*, **422**, 162–171. https://doi.org/10.1016/j.apsusc.2017.05.083.

3. Alamiery, A. (2021) Corrosion inhibition effect of 2-N-phenylamino-5-(3-phenyl-3-oxo-1-propyl)-1,3,4-oxadiazole on mild steel in 1 M hydrochloric acid medium: insight from gravimetric and DFT investigations. *Materials Science and Technology*, **4**, 398–406. https://doi.org/10.1016/j.mset. 2021.09.002.

4. Mohamed, M. G. and Kuo, S. W. (2020) Crown ether-functionalized polybenzoxazine for metal ion adsorption. *Macromolecules*, **53**, 2420–2429. https://doi.org/10.1021/acs.macromol.9b02519.

5. Caldona, E. B., De Leon, A. C. C., Thomas, P. G., Naylor, D. F. III, Pajarito, B. B. and Advincula, R. C. (2017) Superhydrophobic rubber-modified polybenzoxazine/SiO_2 nanocomposite coating with anticorrosion, anti-ice, and superoleophilicity properties. *Industrial & Engineering Chemistry Research*, **56**, 1485–1497. https://doi.org/10.1021/acs.iecr.6b04382.

6. Elaine, A., Alvaro, M., Ferreira, C. A. and Aleman, C. (2009) Polyaniline, polypyrrole and poly(3,4-ethylenedioxythiophene) as additives of organic coatings to prevent corrosion, Surface and Coatings Technology, **203**, 3763–3769. https://doi.org/10.1016/j.surfcoat.2009.06.019.

7. Alamiery, A. A. (2021) Anticorrosion effect of thiosemicarbazide derivative on mild steel in 1 M hydrochloric acid and 0.5 M sulfuric acid:

gravimetrical and theoretical studies. *Materials Science and Technology*, **4**, 263–273. https://doi.org/ 10.1016/j.mset.2021.07.004.

8. Aly, K. I., Amer, A. A., Mahross, M. H., Belal, M. R., Soliman, A. M. and Mohamed, M. G. (2023) Construction of novel polybenzoxazine coating precursor exhibiting excellent anti-corrosion performance through monomer design. *Heliyon*, **9**, e15976. https://doi.org/10.1016/j.heliyon.2023.e15976.

9. Aly, K. I., Mahdy, A., Hegazy, M. A., Al-Muaikel, N. S., Kuo, S. W. and Mohamed, M. G. (2020) Corrosion resistance of mild steel coated with phthalimide-functionalized polybenzoxazines. *Coatings*, **10(11)**, 1114. https://doi.org/10.3390/coatings10111114.

10. Mohamed, M. G., Chang, W. C. and Kuo, S. W. (2022) Crown ether-and benzoxazine-linked porous organic polymers displaying enhanced metal ion and CO_2 capture through solid-state chemical transformation. *Macromolecules*, **55**, 7879–7892. https://doi.org/10.1021/acs.macromol.2c01216.

11. Mohamed, M. G., Chen, T. C. and Kuo, S. W. (2021) Solid-state chemical transformations to enhance gas capture in benzoxazine-linked conjugated microporous polymers. *Macromolecules*, **54**, 5866–5877. https://doi.org/10.1021/acs.macromol.1c00736.

12. Mohamed, M. G., Kuo, S. W., Mahdy, A., Ghayd, I. M. and Aly, K. I. (2020) Bisbenzylidene cyclopentanone and cyclohexanone-functionalized polybenzoxazine nanocomposites: synthesis, characterization, and use for corrosion protection on mild steel. *Materials Today Communications*, **25**, 101418. https://doi.org/10.1016/j.mtcomm.2020.101418.

13. Mohamed, M. G., Li, C. J., Khan, M. A. R., Liaw, C. C., Zhang, K. and Kuo, S. W. (2022) Formaldehyde-free synthesis of fully bio-based multifunctional bisbenzoxazine resins from natural renewable starting materials. *Macromolecules*, **55**, 3106–3115. https://doi.org/10.1021/acs.macromol.2c00417.

14. Mohamed, M. G., Mahdy, A., Obaid, R. J., Hegazy, M. A., Kuo, S. W. and Aly, K. I. (2021) Synthesis and characterization of polybenzoxazine/clay hybrid nanocomposites for UV light shielding and anti-corrosion coatings on mild steel. *Journal of Polymer Research*, **28**, 297. https://doi.org/10.1007/s10965-021-02657-0.

15. Gaikwad, P. S., Krieg, A. S., Deshpande, P. P., Patil, S. U., King, J. A., Maiaru, M. and Odegard, G. M. (2021) Understanding the origin of the low cure shrinkage of polybenzoxazine resin by computational simulation. *ACS Applied Polymer Materials*, **3**, 6407–6415. https://doi.org/10.1021/acsapm.1c01164.

16. Khan, G., Basirun, W. J., Kazi, S. N., Ahmed, P., Magaji, L., Ahmed, S. M. and Badry, A. B. B. M. (2017) Electrochemical investigation on the corrosion inhibition of mild steel by quinazoline Schiff base compounds in hydrochloric acid solution. *Colloids and Surfaces A: Physicochemical and Engineering Aspects*, **502**, 134–145. https://doi.org/10.1016/j.jcis.2017.04.061.

17. Sorkhabi, H. A., Shabani, B., Aligholipour, B. and Seifzadeh, D. (2006) The effect of some Schiff bases on the corrosion of aluminum in hydrochloric acid solution. *Applied Surface Science*, **252**, 4039–4047. https://doi.org/10.1016/j.apsusc.2005.02.148.

18. Chen, N. L., Kong, P. P., Feng, H. X., Wang, Y. Y. and Bai, D. Z. (2019) Corrosion mitigation of chitosan Schiff base for Q235 steel in 1.0 M HCl. *Journal of Bio- and Tribo-Corrosion*, **5**, 1–8. https://doi.org/10.1007/s40735-019-0219-7.

19. Ramanathan, M., Rajendran, G. and Sethumanickam, S. (2022) Eco-friendly chitosan vanillin Schiff base as anti-corrosive agent for mild steel in 1 M HCl and as scale inhibitor for $CaCO_3$. *Journal of Adhesion Science and Technology*, **36,** 23–24. https://doi.org/10.1080/01694243.2022.2066401.

20. Lu, X., Liu, Y., Zhou, C., Zhang, W. and Xin, Z. (2016) Corrosion protection of hydrophobic bisphenol A-based polybenzoxazine coatings on mild steel. *RSC Advances*, **6**, 5805–5811. https://doi.org/10.1039/C5RA22980D.

21. Haubold, T. S., Hartwig, A. and Koschek, K. (2022) Synthesis and application studies of DOPO-based organophosphorous derivatives to modify the thermal behavior of polybenzoxazine. *Polymers*, **14(2)**, 606. https://doi.org/10.3390/polym14030606.

22. Iqbal, M. M., Appasamy, S., Krishnasamy, B., Arumugam, H., Maheshwari, R. V., Vigneshwaran, B. and Muthukaruppan, A. (2023) Development of sustainable polybenzoxazine-based organic–inorganic hybrid nanocomposites for high voltage insulator applications. *Journal of Materials Science: Materials in Electronics*, **34**, 603. https://doi.org/10.1007/s10854-022-09805-2.

23. Tiwari, I., Sharma, P. and Nebhani, L. (2022) Polybenzoxazine—an enticing precursor for engineering heteroatom-doped porous carbon materials with applications beyond energy, environment and catalysis. *Materials Today Chemistry*, **23**, 100734. https://doi.org/10.1016/j.mtchem.2021.100734.

24. Zachariah, S. and Liu, Y. L. (2020) Nanocomposites of polybenzoxazine-functionalized multiwalled carbon nanotubes and polybenzoxazine for anticorrosion application. *Composites Science and Technology*, **194**, 108169. https://doi.org/10.1016/j.compscitech.2020.108169.

25. Chen, C. Y., Chen, W. C., Mohamed, M. G., Chen, Z. Y. and Kuo, S. W. (2023) Highly thermally stable, reversible, and flexible main chain type benzoxazine hybrid incorporating both poly-dimethylsiloxane and double-decker-shaped polyhedral silsesquioxane units through Diels–Alder reaction. *Macromolecular Rapid Communications*, **44**, 2200910. https://doi.org/10.1002/marc.202200910.

26. Zhang, W., Jiang, N., Zhang, T. and Zhang, T. (2021) Preparation and properties of silane-modified cardanol–benzoxazine for hydrophobic coating. *Journal of Elastomers and Plastics*, **53**, 296–310. https://doi.org/10.1177/0095244320933988.

27. Chakravarthy, M., Mohana, K. and Kumar, C. P. (2014) Corrosion inhibition effect and adsorption behaviour of nicotinamide derivatives on mild steel in hydrochloric acid solution. *International Journal of Industrial Chemistry*, **5**, 1–21. https://doi.org/10.1007/s40090-014-0019-3.

28. Mohamed, M. G., Samy, M. M., Mansoure, T. H., Li, C. J., Li, W. C., Chen, J. H. and Kuo, S. W. (2022) Microporous carbon and carbon/metal composite materials derived from bio-benzoxazine-linked precursor for CO_2 capture and energy storage applications. *International Journal of Molecular Sciences*, **23**, 347. https://doi.org/10.3390/ijms23010347.

29. Frisch, M. J., Trucks, G. W., Schlegel, H. B., Scuseria, G. E., Robb, M. A., Cheeseman, J. R., Scalmani, G., Barone, V., Petersson, G. A., Nakatsuji, H., Li, X., Caricato, M., Marenich, A. V., Bloino, J., Janesko, B. G., Gomperts, R., Mennucci, B., Hratchian, H. P., Ortiz, J. V., Izmaylov, A. F., Sonnenberg, J. L., Williams-Young, D., Ding, F., Lipparini, F., Egidi, F., Goings, J., Peng, B., Petrone, A., Henderson, T., Ranasinghe, D., Zakrzewski, V. G., Gao, J., Rega, N., Zheng, G., Liang, W., Hada, M., Ehara, M., Toyota, K., Fukuda, R., Hasegawa, J., Ishida, M., Nakajima, T., Honda, Y., Kitao, O., Nakai, H., Vreven, T., Throssell, K., Montgomery Jr., J. A., Peralta, J. E., Ogliaro, F., Bearpark, M. J., Heyd, J. J., Brothers, E. N., Kudin, K. N., Staroverov, V. N., Keith, T. A., Kobayashi, R., Normand, J., Raghavachari, K., Rendell, A. P., Burant, J. C., Iyengar, S. S., Tomasi, J., Cossi, M., Millam, J. M., Klene, M., Adamo, C., Cammi, R., Ochterski, J. W., Martin, R. L., Morokuma, K., Farkas, O., Foresman, J. B., Fox, D. J. (2016) Gaussian 16, Revision A.03, Gaussi GaussView 6.0.16. *Gaussian Inc., Wallingford CT*.

30. Annaamalai, M. G. L., Maheswaran, G., Ramesh, N., Kamal, C., Venkatesh, G. and Vennila, P. (2018) Investigation of corrosion inhibition of welan gum and neem gum on reinforcing steel embedded in concrete. *International Journal of Electrochemical Science*, **13**, 9981–9998. https://doi.org/10.20964/2018.10.41.

31. Saravana Kumaran, T., Prakasam, A., Venkatesh, G., Vennila, P., Sheena Mary, Y. and Parveen, S. (2023) Design and synthesis of phenylacridine-based organic dyes and its applications in dye-sensitized solar cells. *Russian Journal of Physical Chemistry*, **97**, 2607–2623.

32. Kumaran, T. S., Prakasam, A., Vennila, P., Banu, S. P. and Venkatesh, G. (2021) New carbazole-based organic dyes with various acceptors for dye-sensitized solar cells: synthesis, characterization, DSSCs fabrications and DFT study. *Asian Journal of Chemistry*, **33**, 1541-33, 1550. https://doi.org/10.14233/ajchem.2021.23197.

33. Venkatesh, G., Vennila, P., Govindasamy, C., El Newehy, A. S., Mammadova, K., Cheerlin Mishma, J. N., Manikandan, A. and Balasubramaniyan, S. (2025) Synthesis, characterization, antiproliferative, antibacterial activity, RDG, ELF, LOL molecular docking and physicochemical properties of novel benzodiazepine derivatives. *Journal of Molecular Structure*, **1322**, 140519. https://doi.org/10.1016/j.molstruc.2024.140519.

34. Venkatesh, G., Haseena, S., Vennila, P., Sixto-López, Y., Siva, V., Cheerlin Mishma, J. N., Abul Kalam Azad, S. and Sheena Mary, Y. (2024) Solvation effects, structural, vibrational analysis, chemical reactivity, nanocages, ELF, LOL, docking and MD simulation on sitagliptin. *Chemical Physics Impact*, **8**, 100481. https://doi.org/10.1016/j.chphi.2024.100481.

35. Jayanthi, K., Sivaraju, M., Shanmugasundaram, P. (2023) Enhancing Corrosion Resistance Property of Mild Steel by Benzoxazine Synthesized from Vanillin and Copolymerize with Urethane. *Asian Journal of Chemistry*, **35**, 851-860.

36. Lu, G., Dai, J., Liu, J., Tian, S., Xu, Y., Teng, N. and Liu, X. (2020) A new sight into bio-based polybenzoxazine: from tunable thermal and mechanical properties to excellent marine antifouling performance. *ACS Omega*, **5**, 3763–3773. https://doi.org/10.1021/acsomega.0c00025.

37. Venkaesh, G., Kamal, C., Vennila, P., Kaya, S., Annaamalai, M. G. L. and El Ibrahimi, B. (2022) Sustainable corrosion inhibitor for steel embedded

in concrete by guar gum: electrochemical and theoretical analyses. *Applied Surface Science Advances*, **12**, 100328. https://doi.org/10.1016/j.apsadv.2022.100328.

38. Palanisamy, S. P., Maheswaran, G., Geetha Selvarani, A., Kamal, C. and Venkatesh, G. (2018) Ricinus communis – A green extract for the improvement of anti-corrosion and mechanical properties of reinforcing steel in concrete in chloride media. *Journal of Building Engineering*, **19**, 376–383. https://doi.org/10.1016/j.jobe. 2018.05.020.

39. Palanisamy, S. P., Maheswaran, G., Kamal, C. and Venkatesh, G. (2016) Prosopis juliflora—A green corrosion inhibitor for reinforced steel in concrete. *Research on Chemical Intermediates*, **42**, 7823–7840. https://doi.org/10.1007/s11164-016-2564-1.

40. Periyasamy, K., Sakthivel, P., Venkatesh, G., Vennila, P., Mary, Y. S. and Haseena, S. (2024) Structural and photophysical studies of triphenylamine-based organic dyes for applications in DSSCs: experimental and DFT analysis. *Polycyclic Aromatic Compounds*, **44**, 5314–5337. https://doi.org/10.1080/10406638.2023.2264450.

41. Muthukkumar, M., Rajavel, R., Venkatesh, G. and Vennila, P. (2017) Macrocyclic Schiff base metal complexes derived from isatin: structural activity relationship and DFT calculations. *Tenside Surfactants Detergents*, **54**, 248–259.

42. Jayanthi, K. and Sivaraju, M. (2023) Synthesis and characterization of benzoxazine: urethane copolymer from vanillin with adamantane side chain and its anticorrosive coating on mild steel. *Rasayan Journal of Chemistry*, **16**, 892–904. http://doi.org/10.31788/RJC.2023.1628362.

43. Vennila, P., Kavitha, S., Venkatesh, G., Madhu (2015) Experimental and theoretical investigation of Rosmarinus officinalis leaves extracts as the corrosion inhibitor for mild steel in H_3PO_4 solution; synergistic effect. *Der Pharma Chemica*, **7**, 275–283.